High-pressure/low-temperature neutron scattering of gas inclusion compounds: Progress and prospects

Yusheng Zhao*†, Hongwu Xu*‡, Luke L. Daemen*, Konstantin Lokshin*§, Kimberly T. Tait*, Wendy L. Mao*, Junhua Luo*, Robert P. Currier¶, and Donald D. Hickmott‡

*Los Alamos Neutron Science Center, ‡Earth and Environmental Sciences Division, and ¶Chemistry Division, Los Alamos National Laboratory, Los Alamos, NM 87545; and §Department of Materials Science and Engineering, University of Tennessee, Knoxville, TN 37996

Communicated by Ho-kwang Mao, Carnegie Institution of Washington, Washington, DC, and approved January 5, 2007 (received for review September 14, 2006)

Alternative energy resources such as hydrogen and methane gases are becoming increasingly important for the future economy. A major challenge for using hydrogen is to develop suitable materials to store it under a variety of conditions, which requires systematic studies of the structures, stability, and kinetics of various hydrogen-storing compounds. Neutron scattering is particularly useful for these studies. We have developed high-pressure/low-temperature gas/fluid cells in conjunction with neutron diffraction and inelastic neutron scattering instruments allowing *in situ* and real-time examination of gas uptake/release processes. We studied the formation of methane and hydrogen clathrates, a group of inclusion compounds consisting of frameworks of hydrogen-bonded H_2O molecules with gas molecules trapped inside the cages. Our results reveal that clathrate can store up to four hydrogen molecules in each of its large cages with an intermolecular H_2–H_2 distance of only 2.93 Å. This distance is much shorter than that in the solid/metallic hydrogen (3.78 Å), suggesting a strong densification effect of the clathrate framework on the enclosed hydrogen molecules. The framework-pressurizing effect is striking and may exist in other inclusion compounds such as metal-organic frameworks (MOFs). Owing to the enormous variety and flexibility of their frameworks, inclusion compounds may offer superior properties for storage of hydrogen and/or hydrogen-rich molecules, relative to other types of compounds. We have investigated the hydrogen storage properties of two MOFs, $Cu_3[Co(CN)_6]_2$ and $Cu_3(BTC)_2$ (BTC = benzenetricarboxylate), and our preliminary results demonstrate that the developed neutron-scattering techniques are equally well suited for studying MOFs and other inclusion compounds.

framework-pressurizing effect | hydrogen storage | inelastic neutron scattering | neutron diffraction

Ever-increasing fossil energy consumption and associated global environmental concerns have provoked intensive searches for alternative energy resources. Gas hydrates (clathrates) have been proposed as one of these sources of energy; they are crystalline compounds in which a gas molecule guest is physically incorporated into hydrogen-bonded, cage-like ice host frameworks. Natural clathrates have been found worldwide in permafrost and ocean-floor sediments, as well as in the outer solar system (the moon, comets, Mars, satellites of the gas giant planets), and contain primarily methane (CH_4) and minor amounts of ethane (C_2H_6), propane (C_3H_8), and other gases (isobutene, normal butane, nitrogen, carbon dioxide, and hydrogen sulfide) (1). Naturally occurring hydrates are difficult to study, and much remains to be learned about their crystal structures, bonding mechanisms, thermodynamics, chemical and mechanical stability, reaction with sediments, and kinetics of formation and decomposition.

Hydrogen in the form of H_2, the most abundant gas in the universe, is considered to be one of the most promising alternatives to fossil energy, because it burns cleanly and has high energy efficiency (2). However, incorporation of large amounts of hydrogen into a material that ensures both safe storage and ease of release for energy conversion is one of the most daunting challenges to the realization of the hydrogen economy. The U.S. Department of Energy has set targets for hydrogen storage of 6.0 wt% and/or 1.5 kWh/liter by 2010 and 9.0 wt% and/or 2.7 kWh/liter by 2015. Conventionally, hydrogen has been stored as compressed gas or cryogenic liquid. However, compressed gas stores low contents of hydrogen (only ≈1 wt% at 200–300 bars), and cryogenic liquid requires significant energy (i.e., high cost) to maintain cryogenic conditions. In addition, both methods have safety issues and are not yet practical for mobile applications. Solid-state storage is also being considered as a possible safe and effective way of routinely handling hydrogen, e.g., in the form of metal hydrides (such as $LiBH_4$) (e.g., ref. 3) and via carbon nanotube absorption. Solid-state forms have different properties in terms of balancing high energy density with easy reversibility of adsorption/desorption. For instance, the hydrogen content of $LiBH_4$ is high (18 wt%), but it can only release hydrogen at high temperatures (as high as 900 K). As an alternative, we focus on 3D frameworks of inclusion compounds with cages/cavities that can host hydrogen molecules. Particularly, we emphasize absorption rather than adsorption such that H_2-storage materials may be operational at ambient conditions once stabilized. Inclusion compounds are promising materials because of the vast variety of possible structures and the ability to manipulate their hydrogen storage properties. In addition to energy applications, studying storage of hydrogen in inclusion compounds (specifically clathrates) may provide insights into the nature of hydrogen-rich atmospheres in the large-body interstellar ice embryos postulated to exist during planet formation (4, 5). Moreover, unraveling the gas-encapsulation mechanisms in natural systems (such as methane clathrate) may lay the foundation for designing new synthetic materials for the storage of hydrogen and other gases.

As the lightest element, the hydrogen atom contains only one electron and thus has the weakest x-ray scattering cross-section of all of the elements. In contrast, the scattering power of neutrons does not vary with the number of electrons in an element, and neutron diffraction is much more sensitive to the positions of hydrogen (or its isotopes such as deuterium) and other light elements, making neutron scattering well suited for studying hydrogen-containing or other gas-containing materials. In addition, as neutrons are more penetrating than x-rays, one

Author contributions: Y.Z., L.L.D., K.L., W.L.M., and R.P.C. designed research; Y.Z., H.X., L.L.D., K.L., K.T.T., W.L.M., J.L., and D.D.H. performed research; Y.Z., H.X., L.L.D., K.L., K.T.T., W.L.M., and J.L. analyzed data; and Y.Z., H.X., L.L.D., K.L., K.T.T., W.L.M., R.P.C., and D.D.H. wrote the paper.

The authors declare no conflict of interest.

Freely available online through the PNAS open access option.

Abbreviations: BTC, benzenetricarboxylate; MOF, metal-organic framework; HIPPO, high-pressure preferred-orientation.

†To whom correspondence should be addressed. E-mail: yzhao@lanl.gov.

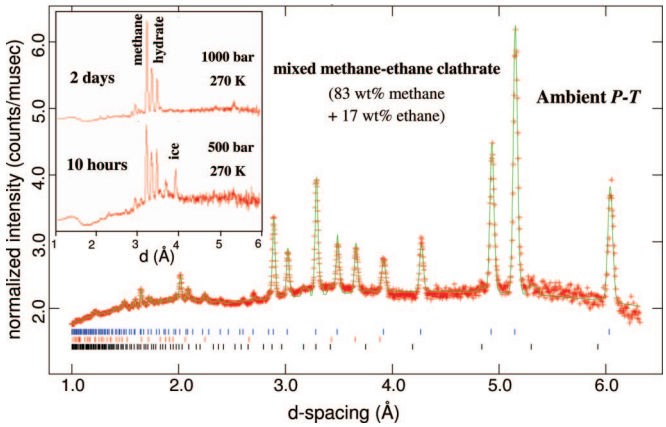

Fig. 1. Fitted neutron diffraction pattern of a mixed methane–ethane sI clathrate (82.93 wt% methane + 17.07 wt% ethane) with minor sII phase and D_2O ice. Data are shown as red plus signs, and the green curve is the best fit to the data. Tick marks below the pattern show the positions of allowed reflections (blue, sI phase; red, ice; black, sII phase). *P-T*, pressure-temperature. (*Inset*) Neutron patterns of methane clathrate formed from ice and D_2 *in situ* in the Al pressure cell. Note that formation of methane clathrate was not complete even after 10 h at 500 bars and 270 K, indicating sluggish formation kinetics compared with hydrogen clathrate.

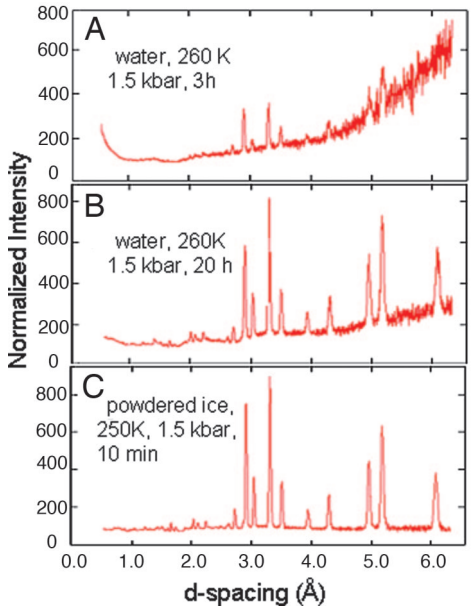

Fig. 2. Neutron diffraction patterns of deuterium clathrates produced from water (*A* and *B*) and powdered ice (*C*), at approximately the same pressure–temperature conditions (11). Note that the formation kinetics of D_2 clathrates formed from ice powder is much faster than from water. [Reproduced with permission from ref. 11 (Copyright 2005, American Institute of Physics).]

can probe samples inside high-pressure vessels, within refrigerators and furnaces, or measure deeply buried local structures within a bulk host material. Hence, neutron scattering in conjunction with variable temperature and pressure capabilities is a powerful tool to monitor the gas uptake/release processes in inclusion compounds, especially for locating the incorporated gas molecules and characterizing their interactions with the host frameworks.

Here, we report neutron diffraction studies of clathrate hydrates, a class of framework compounds consisting of hydrogen-bonded water molecules (1, 6–8). We also report preliminary results on hydrogen storage measurements of $Cu_3[Co(CN)_6]_2$ and $Cu_3(BTC)_2$ (BTC = benzenetricarboxylate), two metal-organic framework (MOF) compounds, and discuss prospects for extending neutron diffraction studies to other inclusion compounds (e.g., ref. 9).

Results and Discussion

We carried out *in situ* and real-time neutron diffraction and inelastic neutron scattering with the high-pressure preferred-orientation (HIPPO) diffractometer and the filter difference spectrometer, respectively, at the Los Alamos Neutron Science Center. Earlier experiments investigated the stability and crystal structures of natural gas hydrates, especially methane, ethane and mixed gas hydrates at various pressures and temperatures, synthesized both *in situ* and *ex situ* (Fig. 1). For *in situ* measurements, polycrystalline ice was prepared by freezing water, crushed with a mortar and pestle at liquid nitrogen temperatures, and then sieved through a stainless-steel mesh to obtain ice particles 300 μm or smaller. The powdered ice was then inserted into the pressure cell; the gas was introduced to the ice and experiments at various pressures and temperatures were performed. To avoid incoherent scattering of H, which contributes to the backgrounds of diffraction patterns, deuterated water and gases were used for the experiments. For example, methane clathrate has been synthesized *in situ* at various pressure/temperature/time conditions (Fig. 1 *Inset*). Our results indicate that the formation kinetics of methane clathrate is much more sluggish than that of hydrogen clathrate (see below). Another method was to synthesize the samples *ex situ* in a high-pressure synthesis apparatus and then load them into the pressure cell. This method reduces the time needed in the neutron beam and additionally portions of the samples could be used for other analyses, such as electron microscopy, mass spectrometry, Raman spectroscopy, and x-ray diffraction. A methane–ethane clathrate sample (Fig. 1) was prepared *ex situ* in an apparatus as described (10) over 26 h with a temperature range of 254–290 K and a pressure range of 20–35 MPa. The sample was then measured at the HIPPO beamline at 200 K and ambient pressure. The final gas concentrations (methane 82.93 wt%, ethane 17.07 wt%, normalized) were measured by gas chromatography, which varied slightly from the initial gas of 80 wt% methane and 20 wt% ethane.

We conducted *in situ* synthesis of deuterium clathrate D_2–D_2O and monitored its stability as a function of pressure and temperature (7). Deuterium clathrate was obtained under 220 MPa of D_2 pressure in the temperature range of 200–270 K, and neutron data were collected during cooling from 200 to 40 K and during heating from 40 to 200 K at ambient pressure. We also used powdered ice (500 μm in diameter) instead of water as a source of D_2O, and our results showed that the formation of deuterium clathrate from ice powder is rapid because of its larger surface area and framework porosity (Fig. 2) (11) (Given the formation of hydrogen clathrate at relatively low pressures, it is possible that large amounts of molecular hydrogen may be entrapped in interstellar ices in the form of the clathrate). The deuterium clathrates synthesized have sII structure (space group *Fd*3*m*), and all of the patterns were analyzed by using the Rietveld method. The sII framework contains eight hexakaidecahedral ($6^4 5^{12}$) cages and 16 smaller dodecahedral (5^{12}) cages per unit cell. The number of D_2 molecules and their distribution in the cages vary systematically with temperature and pressure (Fig. 3). Below 50 K, the guest D_2 molecules are localized, with one D_2 occupying each of the small cages and four D_2 molecules in each of the large cages arranged in a tetrahedral geometry with a D_2–D_2 distance of 2.93(1) Å. Interestingly, the four D_2 molecules in the large cages are oriented toward the centers of the hexagons formed by the framework water molecules, presumably because of the energetic need of minimizing electro-

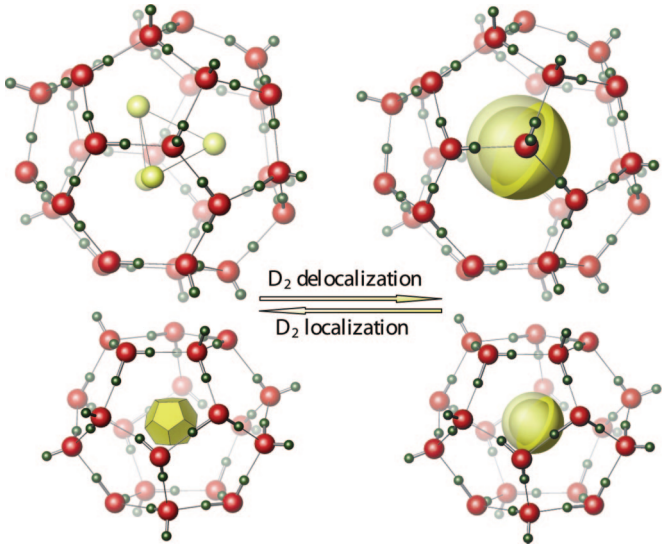

Fig. 3. Structural view of D_2 distribution in the large (*Upper*) and small (*Lower*) cages of deuterium clathrate (7). Oxygen atoms are shown as red spheres, deuterium framework atoms are green, and guest D_2 molecules are yellow. Note that the D_2. . . D_2 separation is the distance between the centers of mass of the two D_2 molecules. Below 50 K, the guest D_2 molecules are localized (*Left*). With increasing temperature, the D_2 molecules can rotate more freely, yielding a nearly spherical D_2 density distribution (*Right*). [Reproduced with permission from ref. 7 (Copyright 2004, American Physical Society).]

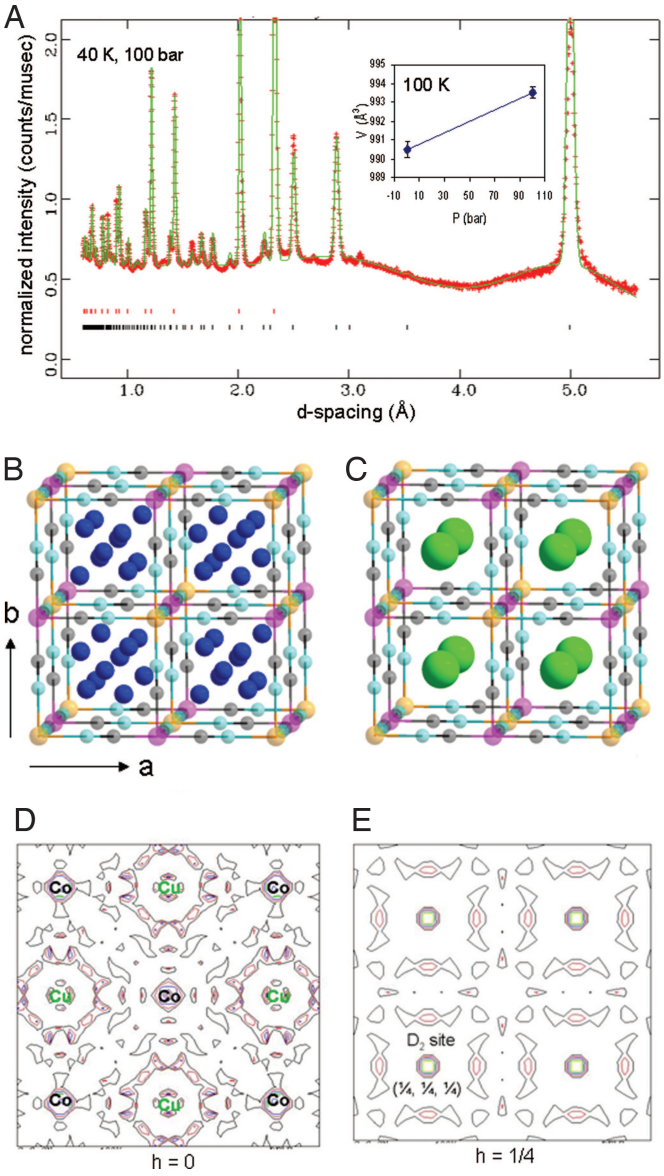

Fig. 4. Neutron diffraction of D_2 sorption in $Cu_3[Co(CN)_6]_2$. (*A*) Fitted neutron diffraction pattern of $Cu_3[Co(CN)_6]_2{\cdot}nD_2$ at 40 K and 10 MPa of D_2 pressure. Data are shown as red plus signs, and the green curve is the best fit to the data. Tick marks below the pattern show the positions of allowed reflections (first row, Al cell; second row, sample). (*Inset*) Increased unit-cell volume under 10 MPa of D_2 pressure at 100 K. (*B*) Crystal structure of $Cu_3[Co(CN)_6]_2{\cdot}9H_2O$ at ambient condition (brown, Cu; pink, Co; black, C; light blue, N; dark blue, water). (*C*) Crystal structure of $Cu_3[Co(CN)_6]_2{\cdot}nH_2$ (green, H_2) showing H_2 at the (¼, ¼, ¼) site (the relatively large green sphere illustrates free-rotation of H_2 molecules in the cages). (*D* and *E*) Difference Fourier nuclear maps showing that the incorporated D_2 molecules mainly occupy the original water site (¼, ¼, ¼) (*E*) with some possibly associated with Cu (*D*). The residual intensities at the Co and Cu sites are probably caused by the limited resolution of our data.

static repulsion. On the other hand, the distance between the four tetrahedrally arranged D_2 molecules (2.93 Å) is small, much shorter than that for solid/metallic hydrogen (3.78 Å) (12). With increasing temperature, D_2 molecules become delocalized, as represented by a uniform distribution of their scattering densities on the surface of a sphere. Correspondingly, the number of D_2 in the large cage gradually decreases to 2.0(2) as temperature rises to 163 K at atmospheric pressure. In contrast, the occupancy of the small cage is constant at one D_2 molecule throughout the temperature range, which is believed to be required for stabilization of the clathrate structure. The clathrate structure tends to collapses as the D_2 starts to escape from the small cage. Upon cooling at 200 MPa, formation of the tetrahedral D_2 cluster in the large cage is complete at 180 K, consistent with the fact that increasing pressure stabilizes clathrate hydrates. Moreover, the distribution of the four D_2 molecules appeared to be similar to that at atmospheric pressure <70 K, when the maximum amount of D_2 was incorporated into the clathrate framework.

This localization–delocalization behavior of D_2 in clathrates is unusual. In particular, multiple D_2 molecules occupying one cage can be delocalized into a freely rotating state with increasing temperature. Further, the intermolecular distance between the four localized D_2 molecules (2.93 Å) is even smaller than that in solid/metallic hydrogen (3.78 Å) that was produced at extremely low temperatures and/or high pressures. This D_2 densification behavior is striking and suggests a strong pressurizing effect that the clathrate framework exerts on the enclosed hydrogen. Similar behavior has been revealed in H_2-adsorbing MOFs, where the intermolecular H_2 distance, obtained by theoretical simulation, can be as short as 3.0 Å (13). Moreover, a recent high-resolution transmission electron microscopy study shows that materials (e.g., iron carbide, iron, and cobalt) encapsulated in carbon nanotubes exhibit severe lattice deformation similar to that under pressures of up to ≈40 GPa (14, 15). Hence, the pressurizing effect may exist in many materials that have nanosized cages/tubes/cavities in which guest phases are encapsulated. Because storage of H_2 usually requires pressure (e.g., compressed H_2 gas), this phenomenon suggests that it is possible to pressurize H_2 into the nanopores of inclusion compounds via absorption, and ideally the frameworks themselves can be stabilized at ambient conditions. The absorptive (versus adsorptive) nature of H_2 with appropriate binding energies would allow incorporation of more H_2 into the frameworks while still maintaining relative fast kinetics of H_2 uptake/release. Hence, inclu-

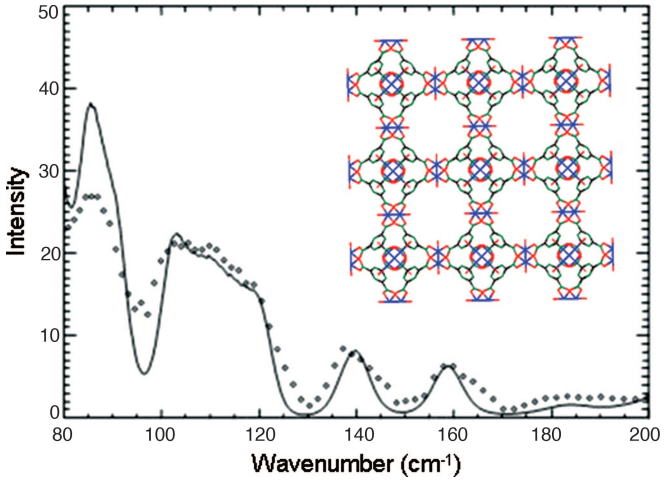

Fig. 5. Low-frequency neutron vibrational spectrum of $Cu_3(BTC)_2$ with its crystal structure shown (*Inset*). $Cu_3(BTC)_2$ has three H_2 equivalents adsorbed at 40 K. The curve is a maximum entropy reconstruction of the spectrum. It enhances some details that are present in the data (dots) but may be not easy to see.

sion compounds with appropriate topologies and cavities may offer another methodology for H_2 storage.

Our *in situ* neutron diffraction studies of hydrogen clathrates have demonstrated the great potential of using the nanocages within inclusion compounds as hosts for hydrogen. Because the conventional clathrate hydrates have only a limited number of framework types (i.e., sI, sII, and sH) (1), this lack of structural diversity limits the ability to tune their cages to encapsulate hydrogen and hydrogen-containing molecules [e.g., $CH_4(H_2)_4$]. However, structural variations in clathrate hydrate frameworks are known. One important class of clathrate variants is the semiclathrates, in which, a portion of the guest molecule chemically binds to the host framework, effectively replacing a water molecule in the lattice. The remainder of the guest is then free to interact with the lattice through van der Waals forces and/or hydrogen bonding. For example, many of the short chain (alkyl)

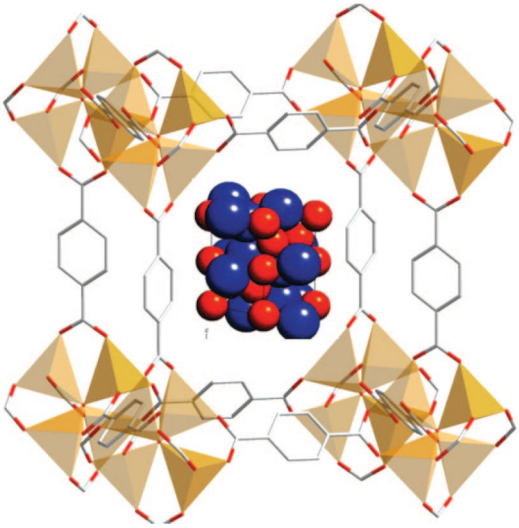

Fig. 6. Structure diagram of a potential hybrid material of the MOF with the $CH_4(H_2)_4$ molecular compound encapsulated into its cage. MOF consists of metal-oxygen clusters (tetrahedra) on the vertices of the lattice and organic linker molecules (hexagons) along its edges, which largely define the size and shape of the cage. Blue balls in $CH_4(H_2)_4$ represent CH_4, and red balls represent H_2.

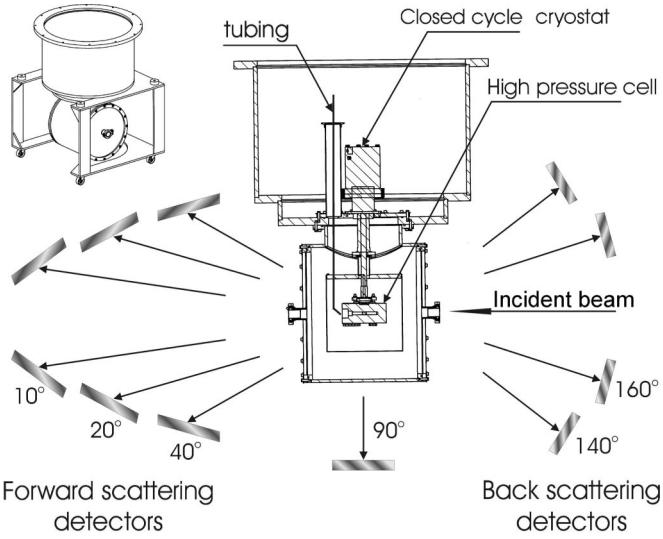

Fig. 7. Schematic general view (in the top-left corner) and the enlarged sectional view of the experimental setup designed for *in situ* high-pressure/low-temperature neutron diffraction at the Los Alamos Neutron Science Center (8). [Reproduced with permission from ref. 8 (Copyright 2005, American Institute of Physics).]

quarternary ammonium salts form stable, ambient pressure semiclathrates (tetra-*n*-butyl-ammonium fluoride forms a semiclathrate that melts at 298 K; and tetra-*n*-butyl ammonium hydroxide semiclathrate melts at 303 K). The increased guest–lattice interactions in the semiclathrates not only enhance thermodynamic stability, they also create extended structures around the central cage-containing sites that can be exploited for hydrogen enclathration. The distorted and enlarged cages are able to trap more hydrogen molecules so that the semiclathrates will be effective as hydrogen storage materials, because of enhanced stability and capacity.

We also explored other families of inclusion compounds, including the recently discovered MOFs, which are among the most promising hydrogen storage candidates (e.g., ref. 9). Through systematic tuning of organic ligands and metal-oxygen clusters at various synthesis conditions, one may obtain framework types with various sizes and shapes of nanopores. Compared with aluminosilicate zeolites, MOFs are much lighter (with densities as low as 0.2 g/cm^3) and, in many cases, more porous (with specific surface areas of up to 4,500–8,000 m^2/g). Moreover, the organic functional groups possess such surface/interface properties as chirality and hydrophilicity, which create favorable sites for hydrogen uptake. Likewise, incorporation of "naked" metal cations (such as Mg^{2+} and Cu^{+}) makes the originally neutral MOF frameworks ionized, thereby polarizing the dihydrogen molecules and resulting in enhanced H_2 sorption. The hydrogen binding energy for these sites is ≈5 kJ/mol (e.g., ref. 16), small enough to enable fast hydrogen uptake/release. In addition, unlike clathrates, the nanoporous frameworks of MOFs are fairly robust, even stable at ambient pressure and high temperatures [e.g., 673 K for MOF-5, $Zn_4O(BDC)_3$, BDC = benzenedicarboxylate]. Thus these compounds are inherently superior as hydrogen storage materials for mobile applications. A number of MOFs have been found to uptake high amounts of H_2 at low temperature (>77 K) and/or high pressure (<10 MPa). For example, MOF-5 can hold up to 4.5 wt% hydrogen at 78 K (17). Further studies are still needed to unravel the mechanisms of hydrogen uptake/release in these materials (e.g., the relative roles of absorption vs. adsorption). *In situ* neutron scattering of

MOFs with various pore sizes and shapes at different pressure/temperature conditions will be particularly useful.

Using the high-pressure/low-temperature cell designed for the clathrate studies, we have recently conducted neutron diffraction experiments on $Cu_3[Co(CN)_6]_2$, an MOF compound, at 10 MPa of D_2 from 40 to 200 K (Fig. 4). This compound is a Prussian blue analogue (space group $Fm\bar{3}m$), in which 1/3 of the $[Co(CN)_6]^{3-}$ sites are vacant, resulting in an aperiodic system of nanopores throughout the structure (Fig. 4*B*). Rietveld analysis (Fig. 4*A*) shows that the cell volume increases from 990.5(4) Å^3 under vacuum to 993.5(3) Å^3 at 10 MPa both at 100 K (Fig. 4*A Inset*), implying incorporation of significant amounts of D_2 into the nanoporous framework. Furthermore, difference Fourier nuclear density maps reveal that the D_2 molecules mainly occupy the interstitial (¼, ¼, ¼) water sites (Fig. 4 *B*, *C*, and *E*) (18) with some possibly associated with the exposed Cu cations (Fig. 4*D*, although data with higher resolution are needed to locate these Cu-related sites). We have also studied the interaction of H_2 with another MOF, $Cu_3(BTC)_2$, at 40–100 K by using inelastic neutron scattering (Fig. 5). This framework is composed of dicopper and BTC units via corner-linking, forming nanosized channels along the a-axes (see Fig. 5 *Inset*). The most striking feature of the neutron vibrational spectrum is the displacement of the rotational level of hydrogen from 118 cm^{-1} down to 86 cm^{-1}, a result of guest–host interactions between H_2 and the framework. Hindering of the $0 \rightarrow 1$ rotation in molecular hydrogen upon adsorption in a number of MOFs (IRMOF-1, IRMOF-8, IRMOF-11, MOF-177) has been observed (18), with shifts from the free rotor value (118 cm^{-1}) to the 80- to 90-cm^{-1} range. This large shift corresponds to the largest barrier to rotation and the strongest binding site for molecular hydrogen. The broad band from 95 to 125 cm^{-1} is resolved into at least three peaks and corresponds to the occupation of other, weaker binding sites for which the $0 \rightarrow 1$ transition is less strongly hindered. The peak at $\approx$160 cm^{-1} has been reported (e.g., ref. 19) and its origin is obscure. It is possible that the $0 \rightarrow 2$ rotational transition might occur below twice the frequency of the fundamental, owing to the existence of the rotational barrier, which affects dramatically the energy-level spacings compared with the free rotor situation (20). Additional vibrational spectra of this compound are being collected with hydrogen injected at high pressure, and more rigorous analysis will yield the binding energies of H_2. Hence, *in situ* neutron diffraction and inelastic scattering are complementary and are well suited for studies of MOFs and other hydrogen-bearing inclusion compounds.

Another area of future research is the development of hybrid hydrogen storage materials with absorptive hydrogen binding. Recent studies using the diamond-anvil cell technique indicate that hydrogen can react with other simple molecular systems (such as CH_4) to form van der Waals compounds at moderate pressures (21). One compound, $CH_4(H_2)_4$, forms at 360 MPa and 86 K and contains 33.4 wt% hydrogen, the highest hydrogen content of any known compound (22). Rather than using the external pressure to produce this compound, one may be able to rely on the inner pressure within the cavity of MOFs (Fig. 6). The same approach may be used for incorporation of other alkane and hydrocarbon molecules into MOFs. The strong pressurizing effect within the nanopores of these hybrid phases increases the likelihood of their stability at more accessible pressure–temperature conditions, and thus their use for practical hydrogen storage. Of course, the technical challenge is to design MOFs that have cages suitable in both size and shape for $CH_4(H_2)_4$ and other molecules. Given the flexibility of the synthetic chemistry of MOF systems, the successful preparation of hybrid compounds is likely. As in the case of hydrogen clathrates, studies of hybrid hydrogen-storage phases require detailed analyses of their structures, kinetics, and stability relations, where *in situ* neutron diffraction under high-pressure and low-temperature conditions is valuable.

Experimental Techniques

We developed a high-pressure/low-temperature fluid/gas cell to perform *in situ* and real-time neutron diffraction and inelastic neutron scattering at the Los Alamos Neutron Science Center's HIPPO and filter difference spectrometer beamlines, respectively (Fig. 7) (8). The pressure cell is constructed of Al-7075 alloy because aluminum has a small cross-section for neutron scattering and maintains reasonably high strength under hydrogen pressures. This cell is powered with a gas/fluid pressure intensifier and a double-stage displex cryostat reaching liquid He temperature. It can hold pressures up to 700 MPa and maintain temperatures down to 20 K on samples as large as 5 cm^3. HIPPO covers a wide range of Q (scattering vector, 0.13–52.4 Å^{-1}) values, and its multiple detectors are configured to provide high counting rates at different diffraction angles. A filter difference spectrometer measures vibrational spectra in the wavenumber range of 40 to 4,000 cm^{-1} with a resolution of 3–5% (using maximum entropy methods for data analysis) and offers several advantages over optical methods (infrared, Raman) such as greater sensitivity to hydrogen and no selection rules. These setups are thus ideal for *in situ* real-time studies of formation/decomposition of hydrogen inclusion compounds as time evolves at various pressure and temperature conditions.

We thank Drs. Ho-kwang Mao and Russell Hemley and two anonymous reviewers for helpful comments and Drs. Sven Vogel and Darrick Williams for assistance with the neutron experiments. This work was supported by the Laboratory Directed Research and Development Program at Los Alamos National Laboratory and has benefited from the use of the Lujan Neutron Scattering Center at the Los Alamos Neutron Science Center, which is funded by the Department of Energy's Office of Basic Energy Sciences. Los Alamos National Laboratory is operated by Los Alamos National Security under Department of Energy Contract DE-AC52-06NA25396.

1. Sloan ED, Jr (1998) *Clathrate Hydrates of Natural Gases* (Dekker, New York), 2nd ed.
2. Schlapbach L, Zuttel A (2001) *Nature* 414:353–358.
3. Grochala W, Edwards PP (2004) *Chem Rev* 104:1283–1315.
4. Sandford SA, Allamandola LJ, Geballe TR (1993) *Science* 262:400–402.
5. Stevenson DJ (1999) *Nature* 400:32.
6. Mao WL, Mao H-k, Goncharov AF, Struzhkin VV, Hemley RJ, Somayazulu M, Zhao Y (2002) *Science* 297:2247–2249.
7. Lokshin KA, Zhao Y, He D, Mao WL, Mao H-k, Hemley RJ (2004) *Phys Rev Lett* 93:125503.
8. Lokshin KA, Zhao Y (2005) *Rev Sci Instrum* 76:063909.
9. Rowsell JLC, Yaghi OM (2005) *Angew Chem Int Ed* 44:4670–4679.
10. Stern LA, Kirby SH, Durham WB (1996) *Science* 273:1843–1848.
11. Lokshin KA, Zhao Y (2005) *Appl Phys Lett* 88:131909.
12. Ishmaev SN, Sadikov IP, Chernyshov AA, Vindryaevskii BA, Sukhoparov VA, Telepnev AS, Kobelev GVJ (1983) *Exp Theor Phys* 84:394–403.
13. Yildirim T, Hartman MR (2005) *Phys Rev Lett* 95:215504.
14. Sun L, Banhart F, Krasheninnikov AV, Rodriguez-Manzo JA, Terrones M, Ajayan PM (2006) *Science* 312:1199–1202.
15. Wang Z, Zhao Y (2006) *Science* 312:1149–1150.
16. Sagara T, Klassen J, Ortony J, Ganz E (2005) *J Chem Phys* 123:014701.
17. Rosi NL, Eckert J, Eddaoudi M, Vodak DT, Kim J, O'Keeffe M, Yaghi OM (2003) *Science* 300:1127–1129.
18. Hartman MR, Peterson VK, Liu Y, Kaye SS, Long JR (2006) *Chem Mater* 18:3221–3224.
19. Rowsell JLC, Eckert J, Yaghi OM (2005) *J Am Chem Soc* 127:14904–14910.
20. Nicol JM, Eckert J, Howard J (1988) *J Phys Chem* 92:7117–7121.
21. Mao WL, Mao H-k (2004) *Proc Natl Acad Sci USA* 101:708–710.
22. Mao WL, Struzhkin VV, Mao H-k, Hemley RJ (2005) *Chem Phys Lett* 402:66–70.